Electronic Supplementary Information

A Minimal Benzo[c][1,2,5]thiadiazole-Based Electron Acceptor as a Third Component Material for Ternary Polymer Solar Cells with Efficiencies Exceeding 16.0%

Yunlong Ma,[a] Xiaobo Zhou,[b] Dongdong Cai,[a] Qisheng Tu,[ac] Wei Ma,[b] and Qingdong Zheng*[a]

[a]State Key Laboratory of Structural Chemistry, Fujian Institute of Research on the Structure of Matter, Chinese Academy of Sciences, 155 Yangqiao West Road, Fuzhou, Fujian 350002, China.

[b]State Key Laboratory for Mechanical Behavior of Materials, Xi'an Jiaotong University, Xi'an, Shaanxi 710049, China.

[c]University of Chinese Academy of Sciences, 19 Yuquan Road, Beijing 100049, China.

E-mail address: qingdongzheng@fjirsm.ac.cn.

Materials

4,7-Bis(5-bromothiophen-2-yl)-5,6-difluorobenzo[c][1,2,5]thiadiazole, J71, ITIC, PM6, Y6 and other materials for this work were purchased from Sigma-Aldrich, Alfa Aesar chemical company, Adamas-beta Ltd., Derthon Optoelectronic Materials Science & Technology Co. Ltd, and eFlexPV limited. Unless otherwise specified, these materials and chemicals were used without any further purification.

General characterization

UV-vis absorption spectra were measured using a Lambda 35 UV/vis spectrophotometer. Photoluminescence spectra were obtained on a Cary spectrophotometer. Time-resolved photoluminescence (TR-PL) measurements were carried out on an FLS980 fluorescence spectrophotometer. DSC measurements were

carried out on DTA404PC. Surface morphology of the active layers was analyzed using a dimension icon AFM in tapping mode. TEM images of the active layers were obtained by a F20 Tecnai instrument operated at an acceleration voltage of 200 kV. Cyclic voltammetry measurements were carried out by using an electrochemical workstation (CHI 604E) in acetonitrile solution with 0.1 M tetrabutylammonium hexafluorophosphate as the supporting electrolyte. Pt plate, Pt wire and $Ag/AgNO_3$ were applied as the working electrode, counter electrode and reference electrode, respectively. HOMO/LUMO energy levels were calculated by using the equation of $E_{HOMO/LUMO} = -(4.82 + \varphi_{ox}/\varphi_{red})$ eV.

Grazing incidence wide angle X-ray scattering (GIWAXS) characterization

GIWAXS measurements were performed at beamline 7.3.3 at the Advanced Light Source. Samples were prepared on Si substrates using identical blend solutions as those used in devices. The 10 keV X-ray beam was incident at a grazing angle of 0.12°-0.16°, selected to maximize the scattering intensity from the samples. The scattered x-rays were detected using a Dectris Pilatus 2M photon counting detector.

Fabrication of inverted PSCs

Indium tin oxide (ITO) glass (sheet resistance = 15 Ω sq^{-1}) was cleaned by sequentially ultrasonicated in detergent, deionized water, acetone, and isopropanol for 15 min each and then drying in an oven at 80 ^oC overnight. The pre-cleaned ITO glasses were UV-cleaned in a UV-ozone chamber for 15 min at room temperature. The ZnO electron transport layers were prepared on the ITO substrate according to previous reported procedures.[1] A chloroform solution that had a fixed J71:ITIC ratio of 1:1 (w/w) at various BTF loadings was spin-coated (3000 r min^{-1}) on the ZnO layer to form a photoactive layer (ca. 130 nm). The concentration of the ternary blend solution is 6 mg/mL for J71. At last, 10 nm of MoO_3 and 100 nm of Ag were deposited onto the photoactive layer through shadow masks by thermal evaporation. The active area of the devices was 4 mm^2. The devices were tested in the glove-box with any encapsulation.

Fabrication of conventional PSCs

The conventional devices were fabricated by using poly(3,4-ethylenedioxythiophene):poly(styrenesulfonate) (PEDOT:PSS) as the hole transport

layer. After oxygen plasma treatment for 4 min, a PEDOT:PSS layer was prepared on the substrates through spin coating at 3500 rpm. Then the PEDOT:PSS substrates were immediately baked at 150 °C in air for 10 min. The PM6:Y6 (1:1.2) blends with and without 10 wt% BTF in donor were fully dissolved in chloroform with a polymer concentration of 6 mg/mL. Before the spin-coating, 1-chloronaphthalene (0.5% volume) was used to optimize the blend film morphology. The mixed solutions were spin-coated onto the PEDOT:PSS-covered substrates at 3500 rpm for 30 s and annealed at 85 ^{o}C for 5 min to prepare the active layers. Then the PDIN solution was spin-coated onto the active layers at 2000 rpm for 30 s. Finally, ~100 nm of Ag was deposited on the top of the PDIN layer through shadow masks by thermal evaporation.

Characterization of PSCs

The devices were measured under AM 1.5 G irradiation (100 mW·cm^{-2}) with an Oriel sol3A simulator (Newport). *J-V* measurements were carried out using a Keithley 2400 source meter. The light intensity for *J-V* measurements was calibrated with a NREL-certified silicon reference cell. EQE data was taken using the QE/IPCE measurement kit (QE-PV-SI) from Newport.

Hole- or electron-only devices fabrication and characterization

Hole- and electron-only devices were fabricated similar to the typical fabrication condition of ternary devices with device structures of ITO/PEDOT:PSS/active layer/Au and ITO /ZnO/active layer/Ca/Al, respectively. The thickness of the film was measured by a Bruker Dektak XT surface profilometer. The *J-V* characterization of the devices was measured by using a computer controlled Keithley 2440 source meter. The SCLC mobilities were calculated by MOTT-Gurney equation[2,3]:

$$J = \frac{9}{8}\varepsilon_r\varepsilon_0\mu\frac{V^2}{L^3}$$

Where ε_r is the relative dielectric constant of the active layer material (assumed to be 3), μ is the hole or electron mobility, ε_0 is the permittivity of empty space (8.85×10^{-12} F m^{-1}), L is the film thickness of the active layer, V is the internal voltage in the device, and $V = V_{appl} - V_{bi}$, where V_{appl} is the applied voltage to the device, and V_{bi} is the built-in voltage due to the relative work function difference between the two electrodes (in

the hole- and electron-only devices, the V_{bi} values are 0.2 and 0.7 V, respectively),[4,5] and J is the current density (A m^{-2}). The hole or electron mobility can be calculated from the slope of the $J^{1/2}$-V curves.

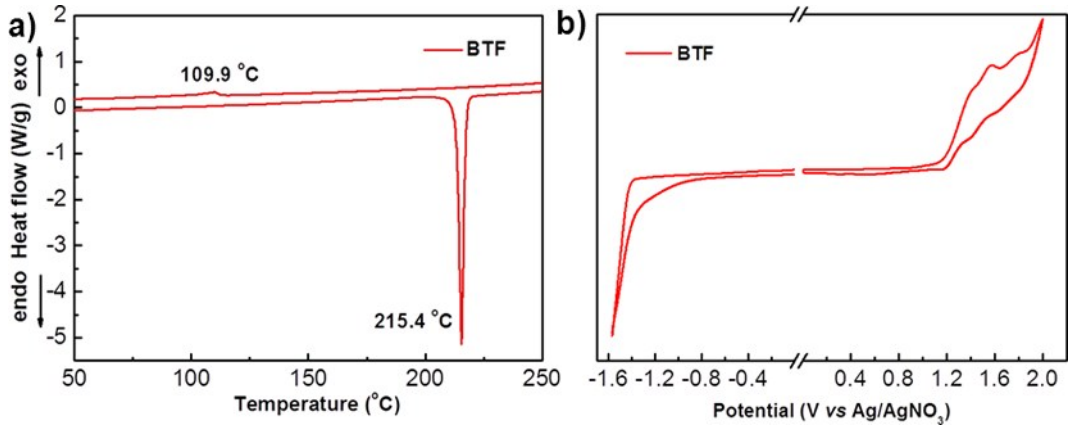

Fig. S1. a) DSC thermogram and b) cyclic voltammogram for BTF.

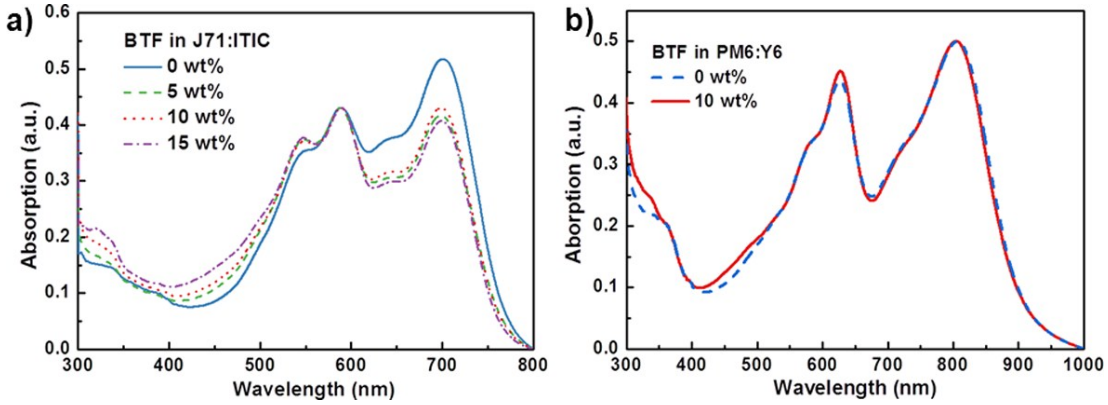

Fig. S2 a) Absorption spectra for J71:ITIC:BTF ternary films with various amounts of BTF; b) absorption spectra for PM6:Y6 blends with and without 10 wt% BTF.

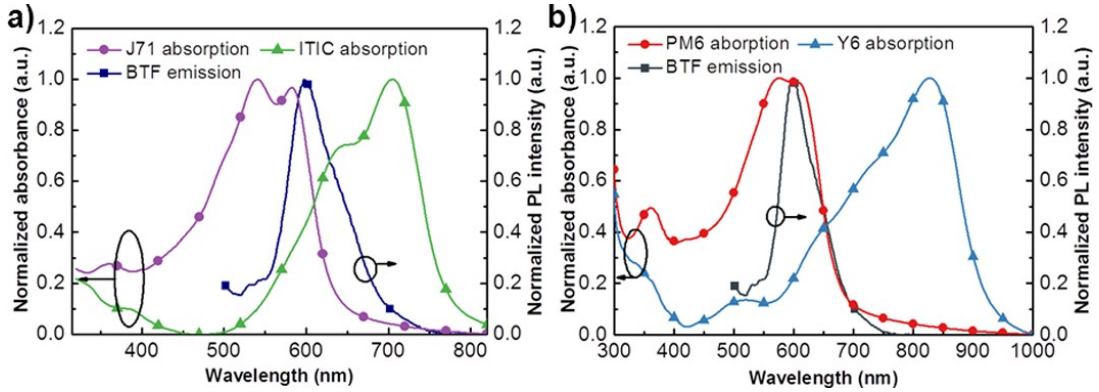

Fig. S3 a) Normalized UV-Vis absorption spectra for J71 and ITIC, and the normalized PL spectrum for BTF film under 460 nm light excitation; b) normalized UV-Vis absorption spectra of PM6 and Y6, and the normalized PL spectrum of BTF film under 460 nm light excitation.

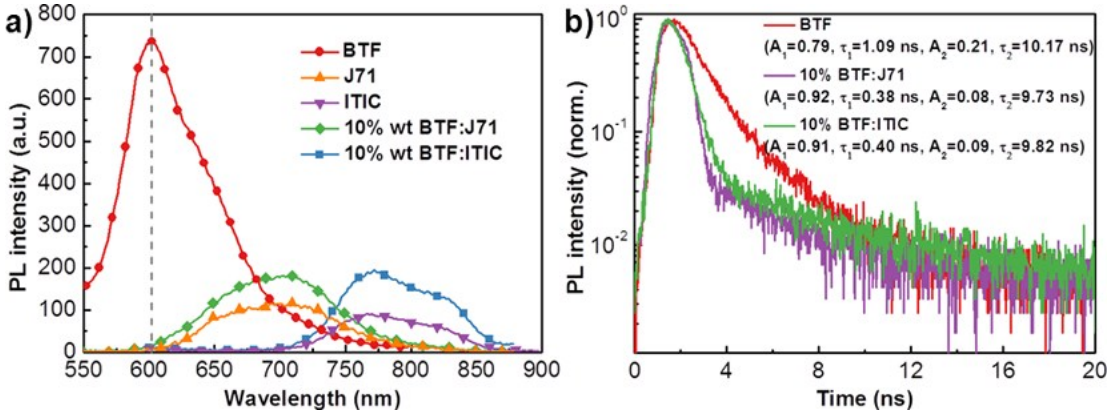

Fig. S4 a) PL spectra for the J71, ITIC, and BTF neat films, and 10wt% J71:BTF film and 10 wt% J71:ITIC film; b) TPL spectra for BTF neat films, 10wt% J71:BTF film and 10 wt% J71:ITIC film.

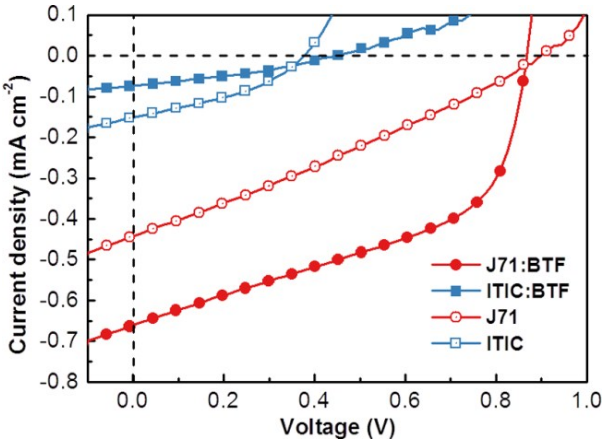

Fig. S5 *J-V* curves for the devices based on J71, ITIC, J71:BTF, and ITIC:BTF films.

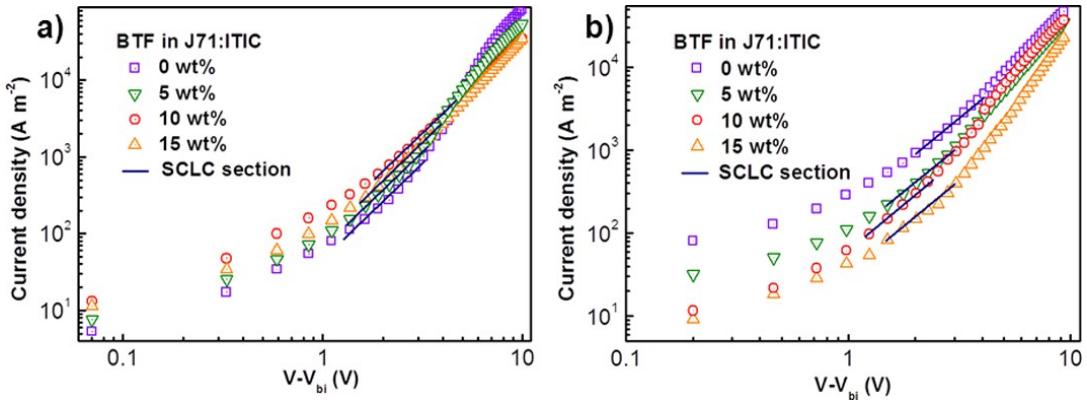

Fig. S6 a) *J-V* curves for the hole-only and b) electron-only of ternary devices with BTF concentrations ranged from 0 to 15 wt%.

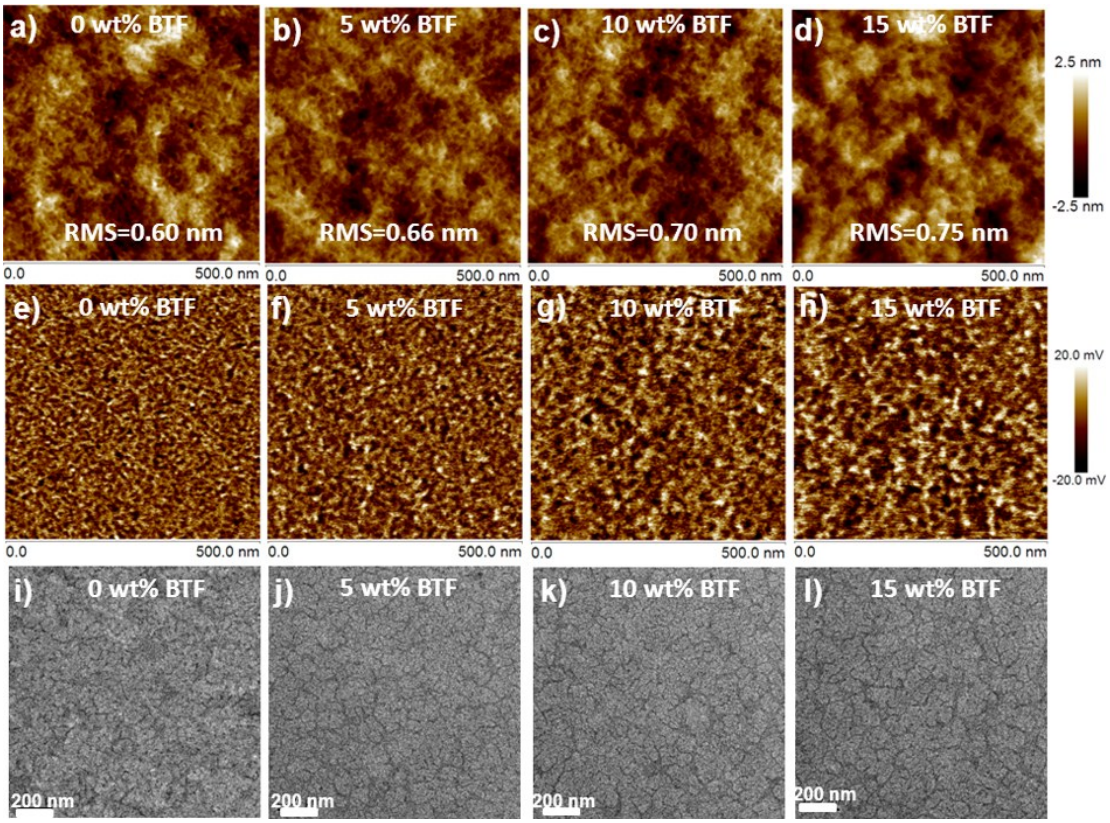

Fig. S7 a-d) AFM topography, e-h) phase, and i-l) TEM images of ternary blends with different BTF contents.

Table S1 Hole and electron mobilities for J71:ITIC:BTF-based devices with different weight percentages of BTF measured by the SCLC method

BTF loading (wt%)	μ_h ($cm^2 V^{-1} s^{-1}$)	μ_e ($cm^2 V^{-1} s^{-1}$)	μ_e/μ_h
0	1.10×10^{-4} (1.04±0.06)	2.20×10^{-4} (2.12±0.09)	2.00
5	1.21×10^{-4} (1.18±0.07)	1.97×10^{-4} (1.85±0.08)	1.63
10	1.40×10^{-4} (1.36±0.05)	1.39×10^{-4} (1.36±0.06)	0.99
15	1.26×10^{-4} (1.23±0.06)	1.18×10^{-4} (1.10±0.07)	0.94

Table S2 Summarized parameters of the ordered structures

BTF loading	π-π stacking		Lamellar stacking	
(wt%)	d-spacing (Å)[a]	CL (Å) (FWHM)[b]	d-spacing (Å)[c]	CL (Å) (FWHM)
0%	3.681	20.583 (0.275 $Å^{-1}$)	20.990	67.344 (0.084 $Å^{-1}$)
5%	3.624	20.759 (0.272 $Å^{-1}$)	20.935	71.136 (0.079 $Å^{-1}$)
10%	3.621	21.563 (0.262 $Å^{-1}$)	21.033	75.537 (0.075 $Å^{-1}$)
15%	3.633	21.796 (0.259 $Å^{-1}$)	21.289	82.979 (0.068 $Å^{-1}$)

[a](010) Diffraction peak along the q_z axis; [b]Coherent length (CL) estimated from the Scherrer equation (CCL=2π*k*/FWHM), in which *k* is the Scherrer factor and FWHM is the full-width at the half-maximum of the peak; [c](100) Diffraction peak along the q_{xy} axis.

Table S3 Photovoltaic parameters for J71:ITIC:BTF-based devices under different annealing temperatures

Annealing temperatures (°C)	V_{oc} (V)	J_{sc} (mA cm^{-2})	FF (%)	PCE (%) [a]
90	0.960	17.02	68.42	11.18 (11.99±0.26)
100	0.956	17.43	69.06	11.51 (11.12±0.46)
110	0.952	18.48	70.03	12.35 (12.14±0.22)
120	0.946	17.42	69.14	11.39 (11.11±0.36)

[a] In parentheses are average PCEs from 8 devices.

Table S4 Photovoltaic parameters for PM6:Y6:BTF-based devices under different annealing temperatures

Annealing temperatures (°C)	V_{oc} (V)	J_{sc} (mA cm^{-2})	FF (%)	PCE (%) [a]
80	0.855	25.88	73.77	16.32 (16.04±0.33)
85	0.853	26.11	74.22	16.53 (16.15±0.36)
90	0.850	26.05	73.03	16.16 (15.89±0.29)
100	0.846	25.94	72.22	15.85 (15.71±0.16)

[a] In parentheses are average PCEs from 8 devices.

References

[S1] Z. Yin, Q. Zheng, S.-C. Chen and D. Cai, *ACS Appl. Mater. Interfaces*, 2013, **5**, 9015-9025.

[S2] P. W. M. Blom, M. J. M. de Jong and M. G. van Munster, *Phys. Rev. B*, 1997, **55**, R656-R659.

[S3] G. G. Malliaras, J. R. Salem, P. J. Brock and C. Scott, *Phys. Rev. B*, 1998, **58**, R13411-R13414.

[S4] X. Guo, N. Zhou, S. J. Lou, J. Smith, D. B. Tice, J. W. Hennek, R. P. Ortiz, J. T. L. Navarrete, S. Li, J. Strzalka, L. X. Chen, R. P. H. Chang, A. Facchetti and T. J. Marks, *Nat. Photonics*, 2013, **7**, 825-833.

[S5] H. Bin, L. Gao, Z.-G. Zhang, Y. Yang, Y. Zhang, C. Zhang, S. Chen, L. Xue, C. Yang, M. Xiao and Y. Li, *Nat. Commun.*, 2016, **7**, 13651.